Published online 11 November 2009

Nucleic Acids Research, 2010, Vol. 38, No. 2 ***499–509***
doi:10.1093/nar/gkp1031

The crystal structure of *Neisseria gonorrhoeae* PriB reveals mechanistic differences among bacterial DNA replication restart pathways

Jinlan Dong[1], Nicholas P. George[2], Katrina L. Duckett[1], Madeleine A. P. DeBeer[1] and Matthew E. Lopper[1,*]

[1]Department of Chemistry, University of Dayton, 300 College Park, Dayton, OH 45469 and [2]Department of Biomolecular Chemistry, University of Wisconsin Medical School, 550 Medical Sciences Center, 1300 University Avenue, Madison, WI 53706, USA

Received September 1, 2009; Revised October 19, 2009; Accepted October 20, 2009

ABSTRACT

Reactivation of repaired DNA replication forks is essential for complete duplication of bacterial genomes. However, not all bacteria encode homologs of the well-studied *Escherichia coli* DNA replication restart primosome proteins, suggesting that there might be distinct mechanistic differences among DNA replication restart pathways in diverse bacteria. Since reactivation of repaired DNA replication forks requires coordinated DNA and protein binding by DNA replication restart primosome proteins, we determined the crystal structure of *Neisseria gonorrhoeae* PriB at 2.7 Å resolution and investigated its ability to physically interact with DNA and PriA helicase. Comparison of the crystal structures of PriB from *N. gonorrhoeae* and *E. coli* reveals a well-conserved homodimeric structure consisting of two oligosaccharide/oligonucleotide-binding (OB) folds. In spite of their overall structural similarity, there is significant species variation in the type and distribution of surface amino acid residues. This correlates with striking differences in the affinity with which each PriB homolog binds single-stranded DNA and PriA helicase. These results provide evidence that mechanisms of DNA replication restart are not identical across diverse species and that these pathways have likely become specialized to meet the needs of individual organisms.

INTRODUCTION

Complete and faithful duplication of cellular genomes is essential for the propagation of life. Accordingly, the process of replicating the DNA genome has evolved to be remarkably efficient. For example, the replication machinery in *Escherichia coli* is capable of synthesizing new DNA at a rate of approximately 1000 nucleotides per second with remarkable fidelity (1). This accomplishment is impressive considering the dynamic nature of the *E. coli* genome. The replication machinery must share the DNA template with other factors, such as those involved in transcription, DNA repair and architectural maintenance. Furthermore, the DNA genome on which all of these factors operate is an imperfect template that is continually marred by DNA damage. Whether arising from the environment or from cellular metabolism, chemical damage to the DNA creates barriers that hinder the progression of the replication machinery (replisome), causing it to stall or dissociate altogether from the DNA template (2). In order to survive, cells must be able to reactivate replisomes that are disrupted in this manner. In bacteria, this process is termed ''DNA replication restart'' and it is driven by a group of proteins called primosome proteins.

Reactivation of disrupted replisomes by DNA replication restart primosome proteins is mechanistically distinct from the initial loading of replisomes onto template DNA (3–6). Initiation of DNA replication is normally restricted to a specific DNA sequence element called an origin of replication. However, advancing replisomes can encounter DNA damage at sites far removed from the origin of replication, so cells require an alternate means of reinitiating DNA replication at non-origin sequences where a replisome has been disrupted. This type of initiation of DNA replication requires recognition of specific DNA structures (such as branched, fork-like structures or D-loop recombination intermediates), as opposed to specific DNA sequences (7,8). In *E. coli*, the primosome proteins that catalyze this process include PriA, PriB, PriC, DnaT and Rep proteins.

A current model for DNA replication restart in *E. coli* involves stepwise assembly of primosome proteins onto

*To whom correspondence should be addressed. Tel: +1 937 229 2674; Fax: +1 937 229 2635; Email: matthew.lopper@notes.udayton.edu

DNA to form a nucleoprotein complex. First, PriA helicase binds to a repaired DNA replication fork. PriB binds to the PriA:DNA complex and stabilizes PriA on the DNA (9). Interactions between PriB and single-stranded DNA (ssDNA) result in stimulation of PriA's helicase activity (10), which is thought to produce a tract of ssDNA onto which the replicative helicase, DnaB, can be reloaded. DnaT is recruited to the ternary PriA:PriB:DNA complex, possibly leading to release of ssDNA that had been bound by PriB (11). Recruitment and reloading of DnaB onto the template DNA results in reactivation of the repaired DNA replication fork, allowing DNA synthesis to resume.

While many studies have focused on DNA replication restart pathways in *E. coli*, relatively little is known of the mechanistic underpinnings and biological importance of DNA replication restart in other bacterial species. Given the broad conservation of *priA* genes among sequenced prokaryotic genomes, it is likely that the general importance of DNA replication restart pathways extends throughout much of the bacterial world. However, many prokaryotic genomes do not harbor the full complement of DNA replication restart primosome genes found in *E. coli*, suggesting that mechanistic details of DNA replication restart, its regulation, and the extent to which cells rely upon it for growth and survival probably vary greatly among diverse bacterial species.

Neisseria gonorrhoeae, the causative agent of gonorrhea, provides a prime example of how DNA replication restart pathways in some bacterial species might differ significantly from those of the well-studied *E. coli* model organism. *N. gonorrhoeae* is a gram-negative bacterium that is highly adapted to survive oxidative damage to its genome incurred by neutrophil attack in infected individuals, suggesting that DNA replication restart pathways might play an expanded and essential role in *N. gonorrhoeae* pathogenicity (12). PriA has been shown to play a critical role in DNA repair in *N. gonorrhoeae* and contributes to the ability of this bacterium to resist the toxic effects of oxidative damaging agents (13). Furthermore, PriA has been identified as an important virulence determinant in *Neisseria meningitidis*, in which it is important for promoting cell growth and resisting oxidative injury (14). Clearly, a direct link exists between the function of DNA replication restart pathways in *Neisseria* species and bacterial growth and survival.

Curiously, while *Neisseria* species encode homologs of *priA* and *priB*, they lack recognizable homologs of *priC* and *dnaT*. This suggests that there might be distinct mechanistic differences between DNA replication restart pathways in *Neisseria* species compared to those that operate in *E. coli*. In this study, we examined the mechanistic underpinnings of DNA replication restart in *N. gonorrhoeae* by solving the crystal structure of *N. gonorrhoeae* PriB and investigating its DNA-binding and PriA-binding activities. Comparison of the *N. gonorrhoeae* and *E. coli* PriB homologs reveals differences in their structure and function that could translate into different mechanisms of DNA replication restart in these diverse bacteria.

MATERIALS AND METHODS

Cloning *priA* and *priB* variants

The *priA* gene of *N. gonorrhoeae* was amplified from strain FA1090 genomic DNA by polymerase chain reaction (PCR) using primers oML172 (5′-GCG TAT TCC ATA TGA TCT ACC ATC GCA TCG CTG TA) and oML173 (5′-GTC ACG GAT CCT CAA GCC TCC TGC GGA TCG AC). The PCR-amplified product was cloned into the pET28b expression vector (Novagen) using NdeI and BamHI restriction sites. The resulting plasmid contains a six-Histidine tag and thrombin cleavage site fused to the 5′ end of *priA*. The cloning of the *priA* gene of *E. coli* was described previously (11). The *priB* gene of *N. gonorrhoeae* was amplified from strain FA1090 genomic DNA by PCR using primers oML226 (5′-GCG TAT TCC ATA TGG GAT TCA CTA ATC TTG TTT CGC) and oML227 (5′-GTC ACG GAT CCT TAA CCT TTA TAT TCT TTA ATA TTT TG). The PCR-amplified product was cloned into the pET28b expression vector (Novagen) using NdeI and BamHI restriction sites. The resulting plasmid contains a six-Histidine tag and thrombin cleavage site fused to the 5′ end of *priB*.

Mutant *priB* genes were constructed using the QuikChange II site-directed mutagenesis kit (Stratagene) according to the manufacturer's instructions. Mutant Y21A was constructed with primers oML266 (5′-CTT TCC CTA TTC GAG CTA CGC CTG CCG GAA TCC CTG) and oML267 (5′-CAG GGA TTC CGG CAG GCG TAG CTC GAA TAG GGA AAG). Mutant K34A was constructed with primers oML268 (5′-GAT ATT ATT TTA GCG CAC GAA TCG TGG C and oML269 (5′-CCA CGA TTC GTG CGC TAA AAT AAT ATC). Mutant E41A was constructed with primers oML270 (5′-GAA TCG TGG CAG GAG GCA AAT GGG CAG CAA TG) and oML271 (5′-CAT TGC TGC CCA TTT GCC TCC TGC CAC GAT TC). Mutant K81A was constructed with primers oML272 (5′-GAA GGT TTT TTA GCT CAA GCA AGC AGA CGT TCC CTG) and oML273 (5′-CAG GGA ACG TCT GCT TGC TTG AGC TAA AAA ACC TTC).

The recombinant *priA* and *priB* genes are under the control of a *T7* promoter for overexpression in hosts harboring T7 polymerase controlled by the *lacUV5* promoter. All plasmids were individually transformed into BL21(DE3) *E. coli* to allow recombinant protein overexpression following induction with isopropyl-β-D-thiogalactopyranoside (IPTG). The fidelity of *priA* and *priB* genes was confirmed by DNA sequencing.

Purification of PriA and PriB variants

Neisseria gonorrhoeae PriA protein was purified from BL21(DE3) *E. coli* harboring the pET28b:*Ngon-priA* plasmid. Cells were grown in Luria Bertani (LB) medium containing 50 μg/ml kanamycin at 37°C until an OD_{600} of 0.6 was reached. Expression of PriA was induced with 0.5 mM IPTG for 4 h and cells were harvested by centrifugation at 5000×*g*. Cells were lysed in 10 mM Hepes pH 7, 10% (v/v) glycerol, 0.5 M NaCl, 0.1 M glucose, 10 mM imidazole, 1 mM β-mercaptoethanol,

1 mM phenylmethylsulfonyl fluoride (PMSF) by sonication on ice. The lysate was clarified by centrifugation at 40 000×*g*. His-tagged PriA was bound to nickel-NTA agarose (Qiagen) and eluted in 10 mM Hepes pH 7, 10% (v/v) glycerol, 0.1 M NaCl, 250 mM imidazole, 1 mM β-mercaptoethanol. The nickel-NTA agarose eluate was dialyzed against 10 mM Hepes pH 7, 10% (v/v) glycerol, 0.1 M NaCl, 1 mM β-mercaptoethanol and incubated with thrombin to remove the His-tag, leaving a Gly-Ser-His sequence at the amino-terminus directly preceding the first methionine residue. Residual His-tagged PriA that was not cleaved by thrombin, as well as contaminating *E. coli* proteins, were depleted by incubating the thrombin-cleaved PriA solution with nickel-NTA agarose. The thrombin-cleaved PriA solution was adjusted to pH 6 with 0.1 M MES and PriA was purified with a HiPrep 16/10 Sepharose SPFF ion exchange column (GE Healthcare) using a linear gradient of NaCl from 0.1 to 1 M in 10 mM MES pH 6, 10% (v/v) glycerol, 1 mM β-mercaptoethanol. PriA fractions were pooled, concentrated to 10 g/l, and stored at −80°C. For pulldown experiments, His-PriA was purified as described above except that thrombin was not added to the nickel-NTA agarose eluate. *E. coli* PriA protein was purified using the same procedure as was used for *N. gonorrhoeae* PriA.

Neisseria gonorrhoeae PriB protein was purified from BL21(DE3) *E. coli* harboring the pET28b:*Ngon-priB* plasmid. Cells were grown in LB medium containing 50 μg/ml kanamycin at 37°C until an OD_{600} of 0.6 was reached. Expression of PriB was induced with 0.5 mM IPTG for 4 h and cells were harvested by centrifugation at 5000 × *g*. Cells were lysed in 10 mM Tris–HCl pH 8.5, 10% (v/v) glycerol, 0.1 M NaCl, 10 mM imidazole, 1 mM β-mercaptoethanol, 1 mM PMSF by sonication on ice. The lysate was clarified by centrifugation at 40 000×*g*. His-tagged PriB was bound to nickel-NTA agarose (Qiagen) and eluted in 10 mM Tris–HCl pH 8.5, 10% (v/v) glycerol, 0.1 M NaCl, 250 mM imidazole, 1 mM β-mercaptoethanol. The nickel-NTA agarose eluate was dialyzed against 10 mM Tris–HCl pH 8.5, 10% (v/v) glycerol, 0.1 M NaCl, 1 mM β-mercaptoethanol and incubated with thrombin to remove the His-tag, leaving a Gly-Ser-His sequence at the amino-terminus directly preceding the first methionine residue. Residual His-tagged PriB that was not cleaved by thrombin, as well as contaminating *E. coli* proteins, were depleted by incubating the thrombin-cleaved PriB solution with nickel-NTA agarose. Thrombin-cleaved PriB was concentrated and purified through a HiPrep HR 16/10 Sephacryl S-100 size exclusion column (GE Healthcare) in 10 mM Tris–HCl pH 8.5, 10% (v/v) glycerol, 0.5 M NaCl, 1 mM β-mercaptoethanol. PriB fractions were pooled, concentrated to 10 g/l, and stored at –80°C. PriB variants were purified using the same procedure used for wild type PriB.

FITC-labeled PriB

Growth and induction of BL21(DE3) *E. coli* harboring the pET28b:*Ngon-priB* plasmid were performed as described above. Cells were lysed in 10 mM Tris–HCl pH 8.5, 10% (v/v) glycerol, 0.1 M NaCl, 10 mM imidazole, 1 mM β-mercaptoethanol, 1 mM PMSF by sonication on ice. The lysate was clarified by centrifugation at 40 000×*g*. His-tagged PriB was bound to nickel-NTA agarose (Qiagen) and eluted in 10 mM Tris–HCl pH 8.5, 10% (v/v) glycerol, 0.1 M NaCl, 250 mM imidazole, 1 mM β-mercaptoethanol. The nickel-NTA agarose eluate was concentrated and purified through a HiPrep HR 16/10 Sephacryl S-100 size exclusion column (GE Healthcare) in 10 mM Tris–HCl pH 8.5, 10% (v/v) glycerol, 0.5 M NaCl, 1 mM β-mercaptoethanol. PriB fractions were pooled, dialyzed against 0.1 M sodium bicarbonate pH 9, 0.5 M NaCl, 10% (v/v) glycerol, 1 mM β-mercaptoethanol, and incubated with a 20-fold molar excess of FITC for 1 h at 25°C in the dark. Residual reactive FITC was quenched with 0.1 M Tris–HCl pH 8.5 for 1 h at 25°C in the dark. FITC-PriB was bound to nickel-NTA agarose beads (Qiagen) and the beads were washed extensively with 10 mM Tris–HCl pH 8.5, 10% (v/v) glycerol, 0.1 M NaCl, 1 mM β-mercaptoethanol to remove unbound FITC. Bound FITC-PriB was eluted in 10 mM Tris–HCl pH 8.5, 10% (v/v) glycerol, 0.1 M NaCl, 0.5 M imidazole, 1 mM β-mercaptoethanol. The nickel-NTA agarose eluate was incubated with thrombin to remove the His-tag from FITC-PriB, leaving a Gly-Ser-His sequence at the amino-terminus directly preceding the first methionine residue. Thrombin-cleaved FITC-PriB was dialyzed against 10 mM Tris–HCl pH 8.5, 10% (v/v) glycerol, 0.5 M NaCl, 1 mM β-mercaptoethanol, and residual His-tagged FITC-PriB that was not cleaved by thrombin, as well as contaminating *E. coli* proteins, were depleted by incubating the FITC-PriB solution with nickel-NTA agarose. FITC-PriB was dialyzed against 10 mM Tris–HCl pH 8.5, 10% (v/v) glycerol, 0.5 M NaCl, 1 mM β-mercaptoethanol, concentrated to 1 g/l, and stored at –80°C.

The degree of labeling (DOL) was determined spectrophotometrically using the following formula:

$$\text{D.O.L.} = (A_{\max} \cdot \text{MW})/([\text{PriB}] \cdot \varepsilon_{\text{dye}}) \quad \textbf{1}$$

where $A_{\max}$ is the wavelength of maximum absorbance for fluorescein (494 nm), MW the molecular weight of PriB (11 445 g/mol), and ε_{dye} the molar extinction coefficient of fluorescein (68 000/M cm). The concentration of PriB was determined using the following formula to correct for the contribution of the FITC dye to the measured absorbance at 280 nm:

$$A_{\text{PriB}} = A_{280} - A_{494}\ (\text{CF}) \quad \textbf{2}$$

where CF = A_{280} free dye/$A_{\max}$ free dye. For FITC, CF = 0.3. The DOL for FITC-PriB determined by this procedure is 0.34 FITC per PriB dimer.

Crystallization of *N. gonorrhoeae* PriB

PriB was dialyzed against 10 mM Tris–HCl pH 8.5, 0.3 M NaCl. Crystals were grown at room temperature by hanging drop vapor diffusion by mixing 1 μl of 10 g/l PriB with 1 μl of well solution comprising 0.1 M sodium

Table 1. X-ray crystallographic data collection, molecular replacement, and structure refinement

Data collection	
Space group	$I4_1$
a (Å)	74.2
b (Å)	74.2
c (Å)	140.4
Resolution (high resolution shell) (Å)	30.0–2.70 (2.75–2.70)
R_{sym} (high resolution shell)[a]	0.072 (0.220)
$I/\sigma(I)$ (high resolution shell)	25.9 (5.5)
Completeness (high resolution shell) (%)	92.8 (65.2)
Redundancy (high resolution shell)	13.3 (10.4)
Refinement	
Resolution (Å)	26.3–2.70
R/R_{free}[b]	0.243/0.288
Number of protein atoms	1626
Average B-factors	
Protein atoms	56.7
Waters	29.5
Root mean square deviations	
Bond lengths (Å)	0.012
Bond angles (°)	1.440
Ramachandran statistics[c]	
Residues in core region	146 (82.5%)
Residues in allowed region	29 (16.4%)
Residues in generously allowed regions	2 (1.1%)
Residues in disallowed regions	0

[a] $R_{sym} = \Sigma_j|I_j - <I>|/\Sigma I_j$, where I_j is the intensity measurement for reflection j and $<I>$ is the mean intensity for multiply recorded reflections.
[b] $R_{work/free} = \Sigma||F_{obs}| - |F_{calc}||/|F_{obs}|$, where the working and free R factors are calculated using the working and free reflection sets, respectively. The free reflections (5% of the total) were held aside throughout refinement.
[c] Ramachandran statistics were generated with PROCHECK (28).

acetate pH 4.2, 4% (w/v) polyethylene glycol 4000. Crystals measuring approximately $100 \times 100 \times 400\,\mu m$ with $I4_1$ symmetry and unit cell dimensions $a = 74.2$ Å, $b = 74.2$ Å, $c = 140.4$ Å, $\alpha = \beta = \gamma = 90°$ grew over a period of ~1 week. Crystals were stabilized by transferring into a cryoprotectant solution comprising 0.1 M sodium acetate pH 4.2, 6% (w/v) PEG 8000, 35% (v/v) glycerol and frozen in liquid nitrogen.

Molecular replacement and model refinement

The crystal structure of *N. gonorrhoeae* PriB was solved at 2.7 Å resolution by molecular replacement with the program Phaser (15) using *E. coli* PriB as a model (Protein Data Bank accession code 1V1Q). Following molecular replacement, model building was performed manually with the program WinCOOT (16). The initial model was improved by rounds of refinement with the program Refmac (17) using tight noncrystallographic symmetry (NCS) restraints between the two monomers of PriB in the asymmetric unit. NCS restraints were lifted in the final stages of refinement so that each PriB monomer could refine independently. The structure was refined to a final R-factor of 0.243 and an R_{free} of 0.288 with good bond geometries. No residues fall into disallowed regions of Ramachandran space (Table 1).

Coordinates

Coordinates have been deposited in the Protein Data Bank (accession code 3K8A).

Fluorescence polarization spectroscopy

Fluorescence polarization spectroscopy was performed at 25°C with a Beacon 2000 fluorescence polarization system (Invitrogen). To measure PriB:DNA interactions, serial dilutions of PriB variants were made into 20 mM Tris–HCl pH 8, 10% (v/v) glycerol, 50 mM NaCl, 1 mM β-mercaptoethanol, 0.1 g/l bovine serum albumin (BSA) and incubated with 1 nM 3′-fluorescein-labeled ssDNA oligonucleotides (fluoro-ssDNA) of varying lengths: 18-mer (5′-AAG CAC AAT TAC CCA CGC), 36-mer (5′-GCC GTG ATC ACC AAT GCA GAT TGA CGA ACC TTT GCC), 45-mer (5′-GCC GTG ATC ACC AAT GCA GAT TGA CGA ACC TTT GCT CCA GTA ACC). Apparent dissociation constants ($K_{d,app}$) were calculated by determining the concentration of titrant required to bind 50% of the fluoro-ssDNA. The unbound state is reported by the fluorescence anisotropy of the fluoro-ssDNA in the absence of PriB. The fully-bound state is reported by the fluorescence anisotropy of the fluoro-ssDNA in the presence of a sufficient concentration of PriB to saturate the fluorescence anisotropy signal. To measure PriA:FITC-PriB interactions, serial dilutions of *E. coli* PriA or *N. gonorrhoeae* PriA were made into 20 mM Tris–HCl pH 8, 4% (v/v) glycerol, 0.1 M NaCl, 1 mM β-mercaptoethanol, 0.1 g/l BSA and incubated with 10 nM FITC-PriB. Apparent dissociation constants were calculated by determining the concentration of titrant required to bind 50% of the FITC-PriB. The unbound state is reported by the fluorescence anisotropy of FITC-PriB in the absence of PriA. The fully bound state is reported by the fluorescence anisotropy of FITC-PriB in the presence of a sufficient concentration of PriA to saturate the fluorescence anisotropy signal. Data are reported in triplicate and associated uncertainties are one standard deviation of the mean.

Pulldown experiments

His-PriA and tagless PriB proteins were diluted to 1 g/l in 10 mM Tris–HCl pH 8, 10% (v/v) glycerol, 0.1 M NaCl, 10 mM imidazole, 1 mM β-mercaptoethanol, 50 g/l BSA and incubated either separately or together at a 1 : 3.5 molar ratio of His-PriA:PriB(dimers) for 30 min at 4°C. Nickel-NTA agarose beads were added to each sample, incubated for 10 min at 4°C, and collected by centrifugation at $21\,130 \times g$ for 2 min at 4°C. The beads were washed several times in 10 mM Tris–HCl pH 8, 10% (v/v) glycerol, 0.1 M NaCl, 10 mM imidazole, 1 mM β-mercaptoethanol, 50 g/l BSA, and collected after each wash by centrifugation at $21\,130 \times g$ for 2 min at 4°C. Pulldown products were eluted by addition of SDS–PAGE sample buffer. The products were resolved through a 13.5% polyacrylamide gel and visualized by Coomassie brilliant blue staining.

RESULTS

Crystal structure of *N. gonorrhoeae* PriB

The *N. gonorrhoeae* PriB protein was crystallized and its structure was determined at 2.7 Å resolution. Molecular replacement was used to generate a readily interpretable electron-density map using the crystal structure of *E. coli* PriB (PDB code 1V1Q) as a search model (Figure 1B). The asymmetric unit contains two molecules of PriB that associate with one another to form a homodimer. The model for the first molecule (chain A) includes amino acid residues 1 through 100 (of 100 total residues) and the model for the second molecule (chain B) includes amino acid residues 1 through 100, plus an amino-terminal Gly-Ser-His sequence that remains following thrombin-cleavage of the amino-terminal His-tag. The model was refined to a final R-factor of 0.243 (R_{free} 0.288) with good bond geometries (Table 1). No residues fall into disallowed regions of Ramachandran space (Table 1).

The *N. gonorrhoeae* PriB homodimer comprises a single structural domain characterized by a flattened β-barrel (Figure 1C). The β-barrel is flanked by α-helices that connect the β3 and β4 strands of each monomer. Collectively, these secondary structural elements are organized into two oligosaccharide/oligonucleotide-binding (OB) folds, one contributed by each monomer of the PriB homodimer. The core of the β-barrel is formed on one side by a six-stranded antiparallel β-sheet that involves three β strands from each molecule of PriB in the homodimer. The opposite side of the β-barrel is formed by two antiparallel β-sheets that are separated by the L_{45} loops. The β4 and β5 strands and the accompanying L_{45} loops extend outward approximately perpendicular to the plane of the β-barrel, while the β2 and β3 strands and the accompanying L_{23} loops fold back along the core of the protein and lie nearly parallel to the long axis of the β-barrel (Figure 1C).

Comparison with *E. coli* PriB

The homodimeric arrangement of OB folds in *N. gonorrhoeae* PriB is well conserved among known PriB homologs. A three-dimensional structure comparison using the DaliLite v.3 server (18) shows that the crystal structure of *N. gonorrhoeae* PriB and various crystal structures of *E. coli* PriB align with r.m.s deviations between 1.3 and 2.6 Å over a range of amino acid residues that encompasses virtually the entire protein. The flattened β-barrel core of *N. gonorrhoeae* PriB is almost identical to that of *E. coli* PriB, although there is a slight rotation of the short α helices that connect the β3 and β4 strands of *N. gonorrhoeae* PriB relative to those of *E. coli* PriB (Figure 1C and D).

The dimerization interface of *N. gonorrhoeae* PriB has similar characteristics to that of *E. coli* PriB. Both PriB homologs have an extensive, highly intertwined dimerization interface that involves significant contributions from the β1 and β3 strands and the L_{23} and L_{45} loops (Figure 1C and D). Approximately 1696 $Å^2$ of each *N. gonorrhoeae* PriB monomer is buried at the dimerization interface (~23% of the total surface area), suggesting that the homodimeric form of *N. gonorrhoeae* PriB represents biologically relevant quaternary structure (19). While the crystal structure of *E. coli* PriB shows the two PriB monomers covalently linked by disulfide bonds (20), there are no equivalent disulfide bonds in the crystal structure of *N. gonorrhoeae* PriB owing to the lack of conservation of the involved cysteine residues.

The largest difference in tertiary structure between the crystal structures of the *N. gonorrhoeae* PriB and *E. coli* PriB homologs is found in the L_{45} loops. The L_{45} loops of *N. gonorrhoeae* PriB are shorter than those of *E. coli* PriB by two amino acid residues but adopt a similar structural arrangement relative to the β-barrel (Figure 1C and D). The L_{45} loops of *E. coli* PriB are more fully extended than those of *N. gonorrhoeae* PriB, but this can be attributed to interactions between *E. coli* PriB and bound ssDNA in the *E. coli* PriB:ssDNA complex. In the apo structure of *E. coli* PriB, the distal amino acid residues of the L_{45} loops lie closer to the core of the β-barrel (21), much as they do in the apo structure of *N. gonorrhoeae* PriB (Figure 1C). The atoms comprising the L_{45} loops in the crystal structure of *N. gonorrhoeae* PriB have an average temperature factor that is substantially greater (83.1 $Å^2$, averaged over the L_{45} loops of both chains) than that of the remainder of the protein (54.4 $Å^2$, averaged over both chains minus the L_{45} loops). This observation is consistent with the hypothesis that the L_{45} loops represent dynamic elements of the PriB structure and is not surprising given that the length and conformation of loop regions vary greatly among OB-fold proteins (22).

Neisseria gonorrhoeae PriB binds single-stranded DNA

Given the overall structural similarity between *N. gonorrhoeae* PriB and *E. coli* PriB, we hypothesized that the mechanism of ssDNA binding is similar between the two PriB homologs. To test this hypothesis, we used fluorescence polarization spectroscopy to probe for a direct, physical interaction between PriB and fluorescein-labeled synthetic ssDNA oligonucleotides of varying lengths. If PriB and ssDNA form a complex, a PriB-dependent increase in fluoro-ssDNA fluorescence anisotropy should be observed due to the greater mass of the PriB:fluoro–ssDNA complex relative to unbound fluoro–ssDNA. When PriB protein was serially diluted and incubated with a fixed concentration of fluoro–ssDNA, we observed a PriB-dependent increase in fluoro-ssDNA fluorescence anisotropy that is saturable with ~5–10 μM PriB (Figure 2). We tested lengths of ssDNA between 18 and 45 bases and observed the highest affinity interaction with a 36-base fluoro-ssDNA oligonucleotide, resulting in an apparent dissociation constant of 475 ± 20 nM (Table 2). The preference of *N. gonorrhoeae* PriB for binding ssDNA of this length is consistent with *E. coli* PriB's apparent site size for ssDNA based on the high-resolution crystal structure of a PriB:ssDNA complex (23).

While our results support the hypothesis that *N. gonorrhoeae* PriB is a ssDNA-binding protein whose function likely mirrors that of the *E. coli* PriB homolog,

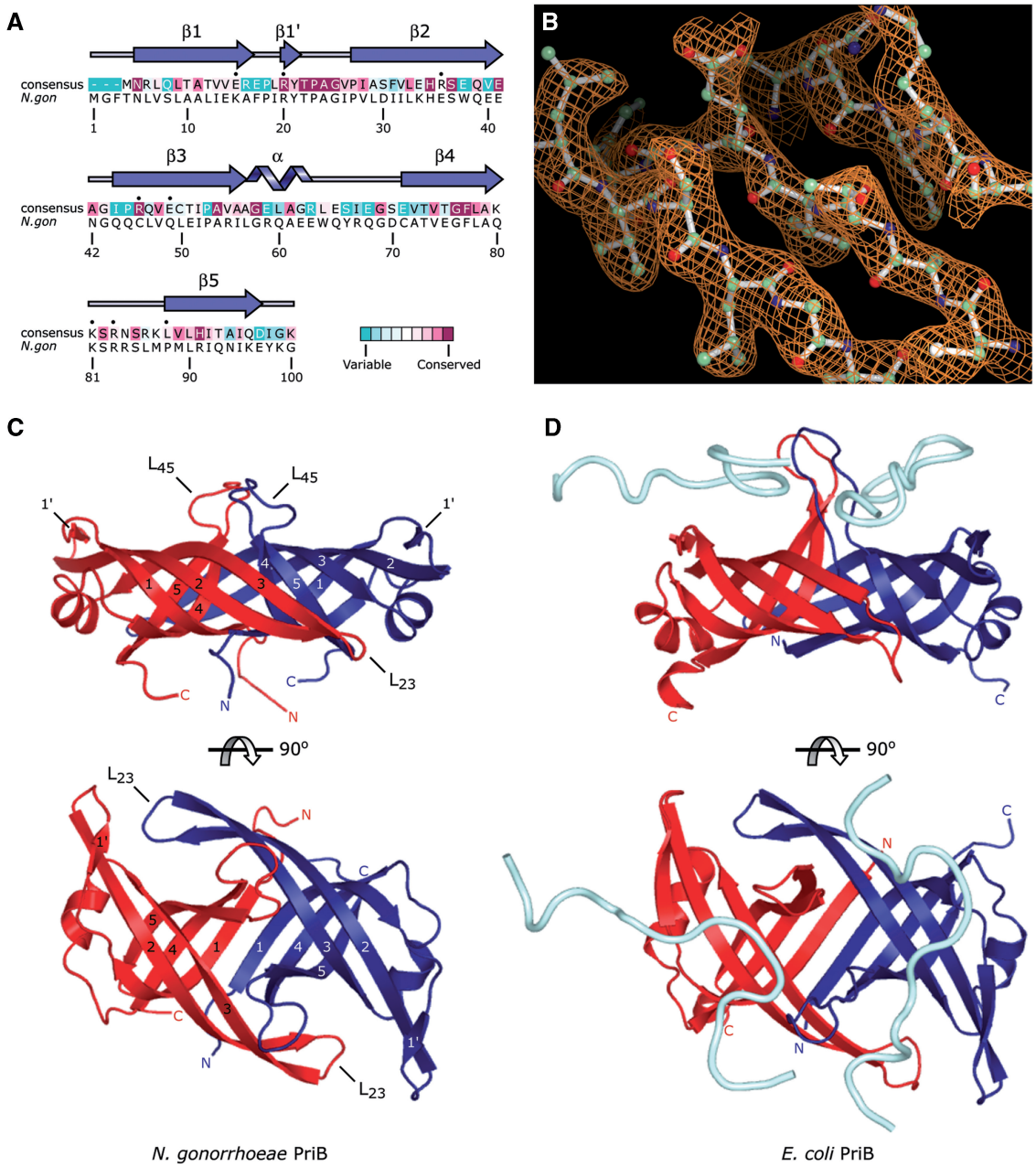

Figure 1. Structure of *N. gonorrhoeae* PriB. (**A**) Alignment of 77 sequenced PriB homologs reveals the degree of variability at each position along the primary sequence. Amino acid residues that are highly variable are colored teal, while highly conserved amino acid residues are colored burgundy (24,25). A consensus sequence was established by determining which amino acid residue is most commonly found at each position relative to the primary sequence of *N. gonorrhoeae* PriB. Residues of the consensus sequence marked with a black dot represent positions at which an aromatic or basic amino acid residue of *E. coli* PriB makes direct contact with ssDNA. Note that these positions do not necessarily correspond to aromatic or basic amino acid residues in the consensus sequence or in *N. gonorrhoeae* PriB. Secondary structural elements of *N. gonorrhoeae* PriB are shown above the corresponding amino acid residues. (**B**) Representative $2F_o - F_c$ electron-density map of three β strands of the PriB β-barrel contoured at 1.4σ above the mean and rendered with PyMOL (26). The stick model overlaying the electron-density map is that of the refined PriB model and is colored according to atom type with carbon atoms colored green, oxygen atoms colored red and nitrogen atoms colored blue. (**C**) Orthogonal views of a ribbon diagram of the crystal structure of *N. gonorrhoeae* PriB. Individual β strands are numbered for each monomer. (**D**) Orthogonal views of a ribbon diagram of the crystal structure of *E. coli* PriB complexed with ssDNA (derived from PDB code 2CCZ) (23). The ribbon diagrams are oriented and colored as in (C), and the ssDNA is rendered as a cyan tube. The ssDNA modeled above the red chain is derived from a symmetry-related molecule.

we were surprised to find from our equilibrium binding experiments that *N. gonorrhoeae* PriB has a 16-fold lower affinity for binding ssDNA compared to *E. coli* PriB (Table 2). Given that *E. coli* PriB and *N. gonorrhoeae* PriB have similar tertiary and quaternary structures, what can account for the difference in the affinity with which *E. coli* PriB and *N. gonorrhoeae* PriB interact with ssDNA? Examination of the crystal structures of *E. coli* PriB and *N. gonorrhoeae* PriB reveals a possible explanation for this dramatic difference in binding affinity. When

the crystal structure of *E. coli* PriB is rendered as a solvent-accessible surface and colored according to electrostatic surface potential, the ssDNA-binding site is delineated by an abundance of positive surface charge potential along the L_{45} loops and adjacent β strands (Figure 3). While the crystal structure of *N. gonorrhoeae* PriB reveals an abundance of Arg and Lys residues along the L_{45} loops and adjacent β strands that are presumably capable of interacting with ssDNA (Figure 4A), there is significantly less solvent-accessible positive surface charge potential associated with this surface compared with the ssDNA-binding site of *E. coli* PriB (Figure 3). The difference in solvent-accessible positive surface charge potential could explain the difference in affinity with which each PriB homolog interacts with ssDNA.

Identification of the single-stranded DNA-binding site

Many of the aromatic and basic amino acid residues of *E. coli* PriB that are important for binding ssDNA are not well conserved in the primary sequences of known PriB homologs (Figure 1A). However, examination of the crystal structures of *E. coli* PriB and *N. gonorrhoeae* PriB reveals that the positions of many of the amino acid residues that are important for binding ssDNA in *E. coli* PriB correspond to basic amino acid residues in *N. gonorrhoeae* PriB that could presumably facilitate physical interactions with ssDNA (Figure 4A). Thus, while these ssDNA-binding amino acid residues have not been well conserved in the primary sequences of these proteins, they appear to have been positionally conserved at the level of protein structure. This led us to hypothesize that the most likely location of the ssDNA-binding site on *N. gonorrhoeae* PriB lies along the L_{45} loops and adjacent β strands and includes amino acid residues such as K15, R20, K34, R55, K81, R83, R84 and R91.

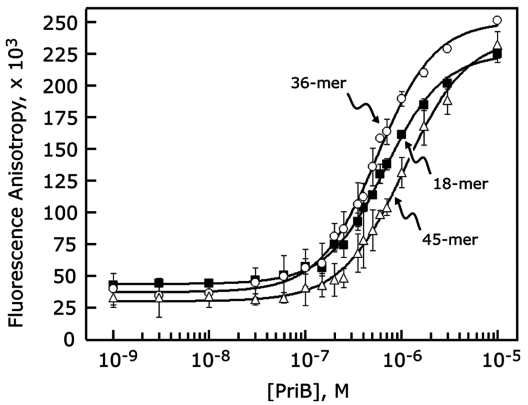

Figure 2. PriB binds ssDNA**.** PriB was serially diluted and incubated with fluorescein-conjugated ssDNA oligonucleotides of varying lengths as described in the 'Materials and Methods' section. Measurements are reported in triplicate and error bars represent 1 SD of the mean.

To test this hypothesis, we generated single alanine-substitution mutants of *N. gonorrhoeae priB* and tested the ability of the PriB variants to interact with ssDNA using fluorescence polarization spectroscopy. As expected, substituting basic amino acid residues that map to the classic ligand-binding surface of PriB's OB folds for alanine results in PriB variants that show significant defects in their ssDNA-binding activity. PriB variants K34A and K81A produce increases in fluorescence anisotropy of a 36-base fluoro-ssDNA oligonucleotide only at high concentrations of protein and the interactions do not saturate even at high concentrations of PriB, precluding determination of an apparent dissociation constant (Figure 4B). These variants migrate through a size exclusion chromatography column in a manner nearly identical to wild type PriB, suggesting that substitution of these surface residues with alanine does not perturb the overall structure of the PriB variants (data not shown). Therefore, it is likely that amino acid residues K34 and K81 make important contributions to ssDNA binding.

We also examined the potential contributions of amino acid residue Y21 to PriB's ssDNA-binding activity. This aromatic amino acid residue occupies a position in the crystal structure of *N. gonorrhoeae* PriB that is not conserved with a ssDNA-binding residue of *E. coli* PriB but is otherwise in close proximity to the presumed ssDNA-binding site. The Y21A PriB variant shows a modest defect in ssDNA binding relative to wild type *N. gonorrhoeae* PriB (Figure 4B). The apparent dissociation constant for the Y21A PriB variant is 641 ± 41 nM, indicating that this variant interacts with ssDNA only 1.3-fold weaker compared to wild type PriB (Table 2). This suggests that amino acid residue Y21 does not likely make significant contributions to ssDNA binding under these conditions. Overall, these observations

Table 2. Apparent dissociation constants for PriB:ssDNA complexes

PriB variant	Apparent dissociation constants ($K_{d,app}$) (nM)			
	18-base ssDNA	30-base ssDNA	36-base ssDNA	45-base ssDNA
Wild type	662 ± 37	574 ± 66	475 ± 20	1018 ± 34
Y21A			641 ± 41	
K34A			>3000[a]	
E41A			139 ± 26	
K81A			>10 000[a]	
E. coli PriB		34.6 ± 7.7[b]		

$K_{d,app}$ values are the mean value derived from three independent experiments and associated uncertainty values are 1 SD of the mean.
[a]For variants for which a $K_{d,app}$ could not be determined due to an inability to obtain saturable binding, a lower limit for the $K_{d,app}$ is reported.
[b]The apparent dissociation constant for an *E. coli* PriB:ssDNA complex was reported previously (20).

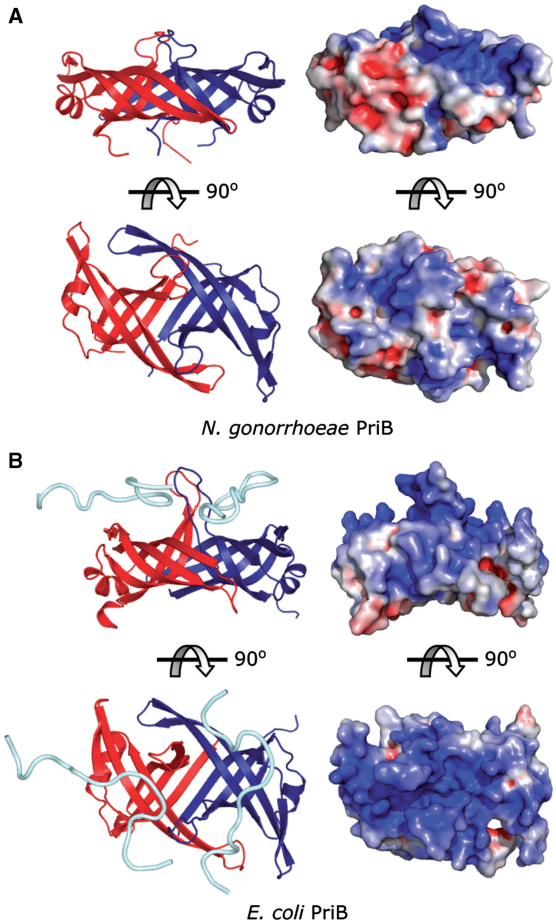

Figure 3. Electrostatic surface potential of PriB. (**A**) Orthogonal views of a ribbon diagram and the solvent-accessible surface of *N. gonorrhoeae* PriB. (**B**) Orthogonal views of a ribbon diagram and the solvent-accessible surface of *E. coli* PriB. The ribbon diagrams are oriented and colored as in Figure 1C and D. Surface potentials were calculated through PyMOL using APBS Tools (27), and the surface views were rendered with PyMOL (26) and are colored according to electrostatic surface potential at ±10 KT/e for positive (blue), negative (red) or neutral (white) charge potential.

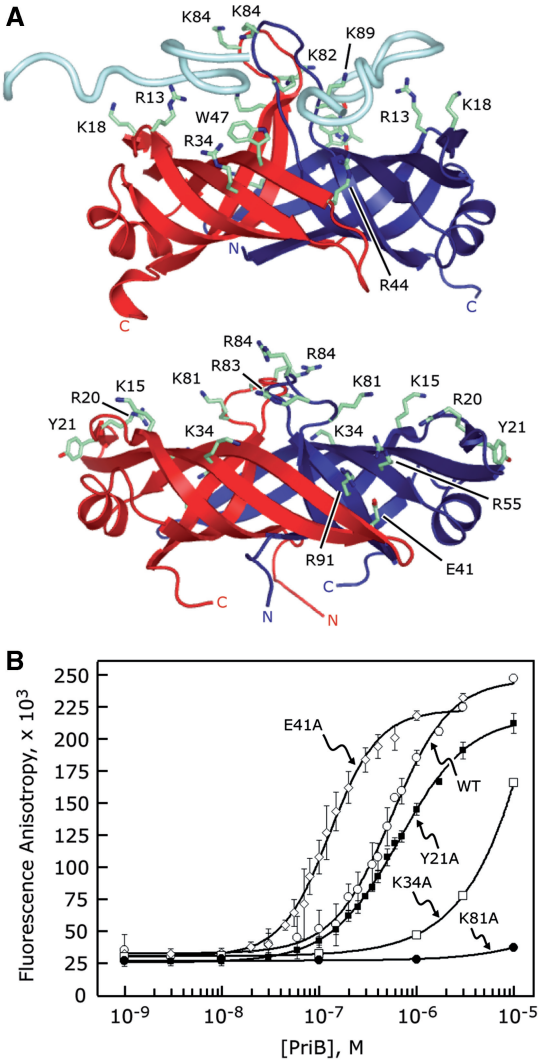

Figure 4. Identification of PriB's binding site for ssDNA. (**A**) Ribbon diagrams of the crystal structures of *E. coli* PriB bound to ssDNA (top) and apo *N. gonorrhoeae* PriB (bottom) oriented and colored as in Figure 1. *E. coli* PriB amino acid residues that are important for binding ssDNA and the analogous residues of *N. gonorrhoeae* PriB are rendered as sticks and colored according to atom type with carbon atoms colored green, oxygen atoms colored red and nitrogen atoms colored blue. (**B**) Wild-type PriB (open circles), Y21A (closed squares), K34A (open squares), E41A (open diamonds) and K81A (closed circles) were serially diluted and incubated with a fluorescein-conjugated 36-base ssDNA oligonucleotide as described in the 'Materials and Methods' section. Measurements are reported in triplicate and error bars represent 1 SD of the mean.

support the hypothesis that *N. gonorrhoeae* PriB binds ssDNA at the classic ligand-binding surface of its OB folds and likely utilizes a mechanism of ssDNA binding that is similar to that used by *E. coli* PriB.

While amino acid residues located on the classic ligand-binding surface of PriB's OB folds appear to be involved in binding ssDNA, we sought to examine the effects of substituting amino acid residue E41 for alanine. Amino acid residue E41 is virtually invariant among known PriB homologs, suggesting that it has an important and well-conserved function. The analogous amino acid residue in *E. coli* PriB, E39, is important for interactions with PriA but does not appear to be involved in binding ssDNA (11). The E39A *E. coli* PriB variant has a 2.4-fold higher affinity for ssDNA than wild type *E. coli* PriB, likely due to eliminating charge repulsion forces between the glutamate side chain and the negatively charged backbone of ssDNA. Likewise, we observed that the E41A *N. gonorrhoeae* PriB variant has a higher affinity for ssDNA than wild type *N. gonorrhoeae* PriB (Figure 4B). The apparent dissociation constant for the E41A *N. gonorrhoeae* PriB variant is 139 ± 26 nM, a 3.4-fold increase in affinity relative to wild type *N. gonorrhoeae* PriB (Table 2). It is likely that the E41 residue of *N. gonorrhoeae* PriB plays a role similar to that of the E39 residue of *E. coli* PriB.

Conservation of the putative PriA-binding pocket

Given the relatively large number of PriB homologs whose genes have been sequenced to date, we analyzed the surface of *N. gonorrhoeae* PriB for regions where amino

acid residues have been well-conserved throughout evolution. A solvent-accessible surface map of *N. gonorrhoeae* PriB that is colored according to amino acid sequence variability reveals two prominent, well-conserved surface patches (Figure 5A). One of these patches includes two notable structural features. One feature is a type II β turn that creates a sharp bend in the polypeptide backbone between the β1′ and β2 strands. The proline and glycine residues that give rise to this hairpin are commonly found in this type of structural element because they help facilitate the 180° reversal of the polypeptide backbone. Hence, the high degree of conservation of the amino acid residues in this region of PriB is likely due to architectural maintenance of the β-barrel. The second feature of this well-conserved surface patch is amino acid residue R20. This basic amino acid residue is positioned on the classic ligand-binding surface of PriB's OB folds and is likely well-conserved because of its ability to facilitate interactions with ssDNA. Consistent with this interpretation, the analogous residue in *E. coli* PriB, K18, appears to make direct contacts with ssDNA in the crystal structure of an *E. coli* PriB:ssDNA complex (23).

The second well-conserved surface patch on PriB lies in a shallow pocket between the two monomers of the PriB homodimer (Figure 5A). In *E. coli*, the physical interaction between PriA and PriB has been partially mapped to this shallow pocket and two amino acid residues that map to this region, R44 and E39, form an ion pair and have been shown to play important roles in the *E. coli* PriA:PriB interaction (11). *Neisseria gonorrhoeae* PriB encodes a glutamate residue, E41, that is positionally conserved with the E39 residue of *E. coli* PriB and we hypothesize that this residue likely plays a role in interactions with PriA (Figure 5B). At the position analogous to that of residue R44 of *E. coli* PriB lies residue C46 in the *N. gonorrhoeae* PriB homolog. However, there are two arginine residues, R55 and R91, positioned near residue C46 in *N. gonorrhoeae* PriB that might serve the same role as R44 of *E. coli* PriB (Figure 5B). Thus, the architecture of this shallow pocket appears to have been remodeled in the time since *E. coli* and *N. gonorrhoeae* shared a common ancestor.

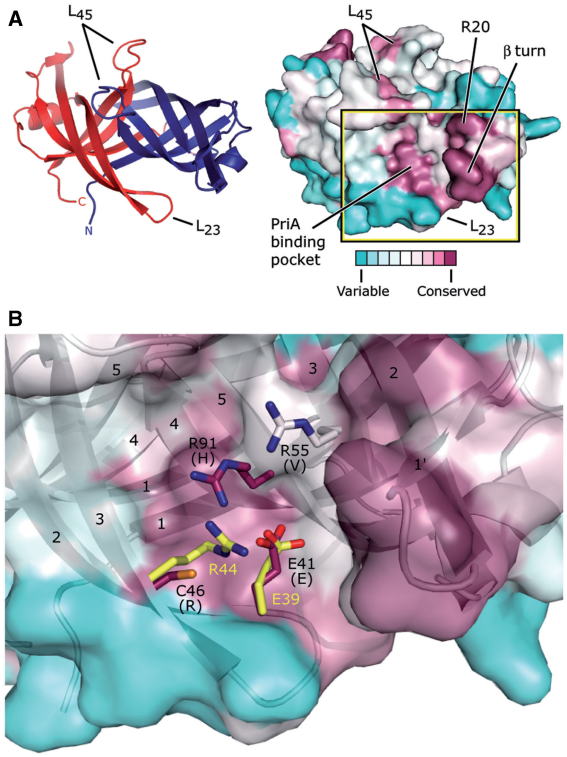

Figure 5. Potential PriA-binding site on PriB. (**A**) Ribbon diagram of the crystal structure of *N. gonorrhoeae* PriB (left) showing frame of reference for the solvent-accessible surface view (right). The ribbon diagram is colored as in Figure 1C and the surface view is colored according to amino acid sequence variability as in Figure 1A. The putative PriA-binding pocket constitutes one of the two main conserved surface patches, and the β turn and amino acid residue R20 constitute the other. (**B**) Expanded, partially-transparent view of the solvent-accessible surface of PriB inscribed by the box in (A). A ribbon diagram of the crystal structure of PriB underlies the surface view. Individual β strands are numbered and amino acid residues located near residue E41 are labeled and rendered as sticks. Carbon atoms are colored according to amino acid sequence variability as in Figure 1A, oxygen atoms are colored red, nitrogen atoms are colored blue and sulfur atoms are colored orange. For each *N. gonorrhoeae* PriB residue rendered as sticks, the amino acid residue that corresponds to the PriB consensus sequence is indicated in parentheses. *E. coli* PriB residues E39 and R44 are superposed with the analogous residues of *N. gonorrhoeae* PriB and are rendered as sticks. The *E. coli* PriB residues are colored according to atom type: carbon atoms are colored yellow, oxygen atoms are colored red and nitrogen atoms are colored blue.

Neisseria gonorrhoeae PriA and PriB form a stable complex

In addition to its role in binding ssDNA, *E. coli* PriB makes important contributions to primosome assembly by forming a complex with PriA that stabilizes PriA on the DNA (9) and enhances its helicase activity (10). However, the physical interaction between *E. coli* PriA and PriB is weak in the absence of DNA, precluding determination of a binding constant (11). To determine if *N. gonorrhoeae* PriA and PriB form a complex and ascertain what effect the remodeled PriA-binding site might have on PriA:PriB interactions, we performed pulldown experiments using His-tagged *N. gonorrhoeae* PriA and tagless *N. gonorrhoeae* PriB to probe for a direct, physical interaction between the two proteins. If PriA and PriB physically interact in a manner that is dependent upon the presence of appropriate DNA substrates, there should be little tagless PriB associated with His-tagged PriA in the pulldown experiment unless DNA is included in the binding reaction. Contrary to expectations, we observed a significant amount of tagless PriB associating with His-tagged PriA in the pulldown experiment that does not require addition of DNA (Figure 6A). This suggests that *N. gonorrhoeae* PriA and PriB form a stable complex in the absence of DNA.

To measure the affinity of the PriA:PriB interaction, we labeled *N. gonorrhoeae* PriB with fluorescein isothiocyanate (FITC) and measured the fluorescence anisotropy of FITC–PriB in the presence and absence of *N. gonorrhoeae* PriA. If the two proteins form a stable complex, a PriA-dependent increase in FITC–PriB fluorescence anisotropy should be observed due to the

greater mass of the PriA:FITC–PriB complex relative to unbound FITC–PriB. When *N. gonorrhoeae* PriA protein was serially diluted and incubated with a fixed concentration of FITC–PriB, we observed a *N. gonorrhoeae* PriA-dependent increase in FITC–PriB fluorescence anisotropy that is saturable with 1–5 μM *N. gonorrhoeae* PriA (Figure 6B). The apparent dissociation constant is 137 ± 16 nM, indicating that a robust PriA:FITC-PriB complex forms under these conditions. Furthermore, the interaction between *N. gonorrhoeae* PriA and FITC-PriB is not affected by the presence of 0.1 g/l DNaseI or 0.1 g/l RNaseA, indicating that the affinity of the interaction is not being augmented by trace levels of nucleic acids that might be contaminating the protein preparations (data not shown).

To determine if the interaction between PriA and FITC–PriB is species-specific, we measured the fluorescence anisotropy of *N. gonorrhoeae* FITC–PriB in the presence and absence of *E. coli* PriA and observed a small increase in fluorescence anisotropy that does not saturate even at high concentrations of *E. coli* PriA (Figure 6B), indicating that *E. coli* PriA and *N. gonorrhoeae* FITC–PriB interact weakly under these conditions. Therefore, the interaction between PriA and FITC–PriB appears to be species-specific.

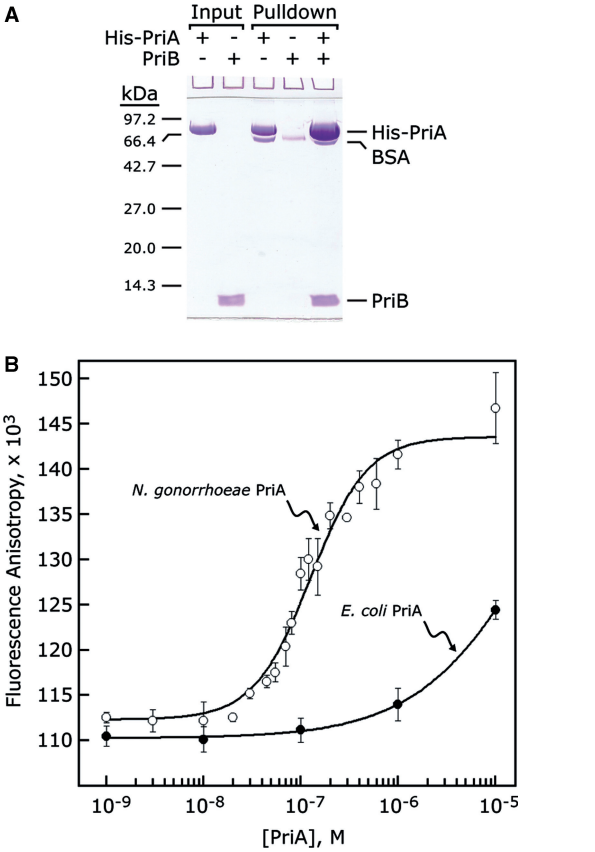

Figure 6. PriA and PriB interact with high affinity. (**A**) His-tagged *N. gonorrhoeae* PriA and tagless *N. gonorrhoeae* PriB were incubated either alone or together and bound to nickel-NTA agarose. Tagless *N. gonorrhoeae* PriB is enriched in the nickel-NTA agarose pulldown fraction only in the presence of His-tagged *N. gonorrhoeae* PriA (**B**) *N. gonorrhoeae* PriA (open circles) and *E. coli* PriA (closed circles) were serially diluted and incubated with FITC-labeled *N. gonorrhoeae* PriB as described in the 'Materials and Methods' section. Measurements are reported in triplicate and error bars represent 1 SD of the mean.

DISCUSSION

We have determined the crystal structure of *N. gonorrhoeae* PriB at 2.7 Å resolution and found that the homodimeric arrangement of the two OB-folds is well conserved with that of the *E. coli* PriB homolog. However, there is significant variation in the surface properties of the two PriB homologs that correlates with dramatically different DNA-binding and PriA-binding activities: *E. coli* PriB has a high affinity interaction with ssDNA and a low affinity interaction with *E. coli* PriA, while *N. gonorrhoeae* PriB has a low affinity interaction with ssDNA and a high affinity interaction with *N. gonorrhoeae* PriA. While the biological consequences of this affinity reversal are unknown with respect to the function of DNA replication restart pathways, our results, coupled with the apparent lack of *priC* and *dnaT* genes in *Neisseria* species, suggest that significant mechanistic differences might exist between *E. coli* and *N. gonorrhoeae* DNA replication restart pathways.

In *E. coli*, the ssDNA-binding activity of PriB is thought to be important for stabilizing PriA on DNA and for enhancing its helicase activity (10). The PriA-stabilizing effect is likely due to increased binding energy made available within a ternary PriA:PriB:DNA complex, while helicase activity enhancement is probably attributed to PriB's ability to bind the ssDNA products of PriA-mediated duplex DNA unwinding. Indeed, when surface residues of *E. coli* PriB that are important for ssDNA binding are substituted for alanine, the mutated PriB variants interact with ssDNA with lower affinity than wild type PriB and lose their ability to enhance PriA's DNA-binding and unwinding activity (10). This suggests that the affinity of *E. coli* PriB for ssDNA is well-tuned to its function in *E. coli* DNA replication restart pathways.

It is unknown if *N. gonorrhoeae* PriB is capable of stabilizing *N. gonorrhoeae* PriA on DNA and enhancing its helicase activity. Given the low affinity with which *N. gonorrhoeae* PriB interacts with ssDNA, it is possible that *N. gonorrhoeae* PriB does not enhance PriA activity in a manner analogous to the *E. coli* model system. On the other hand, the low affinity with which *N. gonorrhoeae* PriB binds ssDNA might be compensated for by the high affinity with which it binds PriA, thereby producing a stable PriA:PriB:DNA ternary complex analogous to the *E. coli* PriA:PriB:DNA ternary complex. If the overall stability of the PriA:PriB:DNA ternary complex is equivalent between the two species, what might be the advantage of tuning the affinities with which individual components interact with one another? One possible explanation for the high affinity interaction between *N. gonorrhoeae* PriA and PriB is that it could allow *N. gonorrhoeae* cells to respond more quickly to disruptions in DNA replication by maintaining preformed PriA:PriB complexes. This could presumably

benefit an organism such as *N. gonorrhoeae* whose natural habitat is replete with DNA damaging agents. Furthermore, since there is evidence that *E. coli* DnaT functions to dissociate ssDNA from *E. coli* PriB, perhaps to facilitate DnaB loading onto the template DNA (11), an organism that lacks DnaT might require its PriB homolog to have a lower affinity for ssDNA to allow for dissociation of ssDNA from PriB without assistance. Further experimentation will be required to address these questions.

ACCESSION NUMBER

3K8A.

ACKNOWLEDGEMENTS

X-ray diffraction data were collected at the Advanced Photon Source Life Sciences Collaborative Access Team (LS-CAT) Beamline 21-ID-F at the Argonne National Laboratories. The authors are grateful to James L. Keck for critical review of the manuscript.

FUNDING

University of Dayton Research Council (3782350005 to M.E.L.); University of Dayton Graduate School (J.D.); University of Dayton Department of Chemistry (K.L.D.). Funding for open access charge: University of Dayton Department of Chemistry start-up funds.

Conflict of interest statement. None declared.

REFERENCES

1. Baker,T.A. and Bell,S.P. (1998) Polymerases and the replisome: machines within machines. *Cell*, **92**, 295–305.
2. Kreuzer,K.N. (2005) Interplay between DNA replication and recombination in prokaryotes. *Annu. Rev. Microbiol.*, **59**, 43–67.
3. Michel,B., Grompone,G., Flores,M.J. and Bidnenko,V. (2004) Multiple pathways process stalled replication forks. *Proc. Natl Acad. Sci. USA*, **101**, 12783–12788.
4. Sandler,S.J. and Marians,K.J. (2000) Role of PriA in replication fork reactivation in Escherichia coli. *J. Bacteriol.*, **182**, 9–13.
5. Cox,M.M. (2002) The nonmutagenic repair of broken replication forks via recombination. *Mutat. Res.*, **510**, 107–120.
6. McGlynn,P. and Lloyd,R.G. (2002) Recombinational repair and restart of damaged replication forks. *Nat. Rev. Mol. Cell Biol.*, **3**, 859–870.
7. McGlynn,P., Al-Deib,A.A., Liu,J., Marians,K.J. and Lloyd,R.G. (1997) The DNA replication protein PriA and the recombination protein RecG bind D-loops. *J. Mol. Biol.*, **270**, 212–221.
8. Nurse,P., Liu,J. and Marians,K.J. (1999) Two modes of PriA binding to DNA. *J. Biol. Chem.*, **274**, 25026–25032.
9. Ng,J.Y. and Marians,K.J. (1996) The ordered assembly of the phiX174-type primosome. I. Isolation and identification of intermediate protein-DNA complexes. *J. Biol. Chem.*, **271**, 15642–15648.
10. Cadman,C.J., Lopper,M., Moon,P.B., Keck,J.L. and McGlynn,P. (2005) PriB stimulates PriA helicase via an interaction with single-stranded DNA. *J. Biol. Chem.*, **280**, 39693–39700.
11. Lopper,M., Boonsombat,R., Sandler,S.J. and Keck,J.L. (2007) A hand-off mechanism for primosome assembly in replication restart. *Mol. Cell*, **26**, 781–793.
12. Shafer,W.M. and Rest,R.F. (1989) Interactions of gonococci with phagocytic cells. *Annu. Rev. Microbiol.*, **43**, 121–145.
13. Kline,K.A. and Seifert,H.S. (2005) Mutation of the priA gene of Neisseria gonorrhoeae affects DNA transformation and DNA repair. *J. Bacteriol.*, **187**, 5347–5355.
14. Tala,A., De Stefano,M., Bucci,C. and Alifano,P. (2008) Reverse transcriptase-PCR differential display analysis of meningococcal transcripts during infection of human cells: up-regulation of priA and its role in intracellular replication. *BMC Microbiol.*, **8**, 131.
15. McCoy,A.J., Grosse-Kunstleve,R.W., Adams,P.D., Winn,M.D., Storoni,L.C. and Read,R.J. (2007) Phaser crystallographic software. *J. Appl. Cryst.*, **40**, 658–674.
16. Emsley,P. and Cowtan,K. (2004) Coot: model-building tools for molecular graphics. *Acta Crystallogr. D Biol. Crystallogr.*, **60**, 2126–2132.
17. Winn,M.D., Isupov,M.N. and Murshudov,G.N. (2001) Use of TLS parameters to model anisotropic displacements in macromolecular refinement. *Acta Crystallogr. D Biol. Crystallogr.*, **57**, 122–133.
18. Holm,L., Kaariainen,S., Rosenstrom,P. and Schenkel,A. (2008) Searching protein structure databases with DaliLite v.3. *Bioinformatics*, **24**, 2780–2781.
19. Nooren,I.M. and Thornton,J.M. (2003) Diversity of protein-protein interactions. *Embo J.*, **22**, 3486–3492.
20. Lopper,M., Holton,J.M. and Keck,J.L. (2004) Crystal structure of PriB, a component of the Escherichia coli replication restart primosome. *Structure (Camb)*, **12**, 1967–1975.
21. Liu,J.H., Chang,T.W., Huang,C.Y., Chen,S.U., Wu,H.N., Chang,M.C. and Hsiao,C.D. (2004) Crystal structure of PriB-a primosomal DNA replication protein of Escherichia coli. *J. Biol. Chem.*, **279**, 50465–50471.
22. Theobald,D.L., Mitton-Fry,R.M. and Wuttke,D.S. (2003) Nucleic acid recognition by OB-fold proteins. *Annu. Rev. Biophys. Biomol. Struct.*, **32**, 115–133.
23. Huang,C.Y., Hsu,C.H., Sun,Y.J., Wu,H.N. and Hsiao,C.D. (2006) Complexed crystal structure of replication restart primosome protein PriB reveals a novel single-stranded DNA-binding mode. *Nucleic Acids Res.*, **34**, 3878–3886.
24. Landau,M., Mayrose,I., Rosenberg,Y., Glaser,F., Martz,E., Pupko,T. and Ben-Tal,N. (2005) ConSurf 2005: the projection of evolutionary conservation scores of residues on protein structures. *Nucleic Acids Res.*, **33**, W299–302.
25. Glaser,F., Pupko,T., Paz,I., Bell,R.E., Bechor-Shental,D., Martz,E. and Ben-Tal,N. (2003) ConSurf: identification of functional regions in proteins by surface-mapping of phylogenetic information. *Bioinformatics*, **19**, 163–164.
26. DeLano,W.L. (2002) The PyMOL Molecular Graphics System. DeLano Scientific, San Carlos, CA, USA.
27. Baker,N.A., Sept,D., Joseph,S., Holst,M.J. and McCammon,J.A. (2001) Electrostatics of nanosystems: application to microtubules and the ribosome. *Proc. Natl Acad. Sci. USA*, **98**, 10037–10041.
28. Laskowski,R.A., MacArthur,M.W., Moss,D.S. and Thornton,J.M. (1993) PROCHECK: a program to check the stereochemical quality of protein structures. *J. Appl. Cryst.*, **26**, 283–291.